Analytical dynamic modeling of fast trilayer polypyrrole bending actuators

# Analytical dynamic modeling of fast trilayer polypyrrole bending actuators

**Amir Ali Amiri Moghadam**[1,3]**, Majid Moavenian**[1]**, Keivan Torabi**[2] **and Masoud Tahani**[1]

[1] Faculty of Engineering, Department of Mechanical Engineering, Ferdowsi University of Mashhad, P.O. Box: 9177948944-11, Iran
[2] Faculty of Engineering, Department of Mechanical Engineering, University of Kashan, P.O. Box: 87317-51167, Iran

E-mail: am_am302@stu-mail.um.ac.ir, moaven@um.ac.ir, kvntrb@kashanu.ac.ir and mtahani@.um.ac.ir

## Abstract

Analytical modeling of conjugated polymer actuators with complicated electro-chemo-mechanical dynamics is an interesting area for research, due to the wide range of applications including biomimetic robots and biomedical devices. Although there have been extensive reports on modeling the electrochemical dynamics of polypyrrole (PPy) bending actuators, mechanical dynamics modeling of the actuators remains unexplored. PPy actuators can operate with low voltage while producing large displacement in comparison to robotic joints, they do not have friction or backlash, but they suffer from some disadvantages such as creep and hysteresis. In this paper, a complete analytical dynamic model for fast trilayer polypyrrole bending actuators has been proposed and named the analytical multi-domain dynamic actuator (AMDDA) model. First an electrical admittance model of the actuator will be obtained based on a distributed $RC$ line; subsequently a proper mechanical dynamic model will be derived, based on Hamilton's principle. The purposed modeling approach will be validated based on recently published experimental results.

(Some figures may appear in colour only in the online journal)

## Introduction

There is an increasing requirement for a new generation of actuators which can be used in devices such as artificial organs, micro-robots, human-like robots, and medical applications. Up to now, a great deal of research has been carried out on developing new actuators such as shape memory alloys, piezoelectric actuators, magnetostrictive actuators, contractile polymer actuators, and electrostatic actuators [1, 2]. The main disadvantages of these actuators are low efficiency, high electrical power, and low strain generation [2]. Electroactive polymers (EAPs) seem to be among the best possible candidates for application in micromanipulation systems since they produce reasonable strain under low input voltage. EAPs are a relatively new class of materials which can be used as both sensors and actuators [3]. Conductive polymer

[3] Author to whom any correspondence should be addressed.

(CP) and ionic metal polymer composite (IPMC) are among the electroactive polymer materials which exhibit interesting sensing and actuating behavior [4]. In this study we will focus on dynamic modeling of a trilayer conductive polymer actuator based on polypyrrole [5, 6].

The main process responsible for volumetric change and the resulting actuation ability of conjugated polymer actuators is reduction/oxidation (RedOx). Thus, based on different fabrication forms, different configurations of the actuators can be obtained, namely linear extenders, bilayer benders, and trilayer benders [7–9]. By applying a voltage to a trilayer polymer actuator, the polypyrrole (PPy) layer on the anode side is oxidized while that on the cathode side is reduced. Ions can transfer inside the conjugated polymer actuator based on two main mechanisms, namely diffusion and drift [10]. There are many reports in the literature on the potential application of electroactive polymer (EAP) in different robotic systems. Chen

*et al* [11] reported the modeling of a robotic fish propelled by an ionic-polymer–metal composite (IPMC) actuator. Jager *et al* [12] reviewed the current status of microactuators based on EPA. They described microfabrication of these actuators plus the possible application of them in microsystems. We have detailed the dynamic modeling and control of a soft micro-robot based on conjugated polymer actuators which could be used in micromanipulation systems [13].

Trilayer polypyrrole actuators, which could operate both in air and in a liquid environment are promising materials for application in micromanipulation systems [14–16]. However, before they can be utilized in practical applications, it is essential to understand their dynamics. In particular, in applying a fast trilayer polypyrrole actuator, the proper mechanical dynamics [16] must be considered. Most of the available models in the literature of conductive polymer actuators have focused on static operating conditions [17, 18, 24, 38]; however, application of these materials in practical devices requires a dynamic modeling approach. Although Fang *et al* [6] have proposed a dynamic model for trilayer polymer actuators, but they have only used the electrical admittance model of the actuator and ignored the mechanical dynamics. The main contributions on modeling the mechanical dynamics of fast trilayer polypyrrole actuators are mainly limited to presenting and evaluating the experimental data [14–16, 19]. In our previous work we have applied the finite element method for the modeling of polymer actuators [20]. In this paper we will develop a complete analytical dynamic model between the input voltage and output displacement of a fast trilayer polypyrrole actuator. Our complete electro-chemo-mechanical dynamic model consists of an electrical admittance model based on a distributed $RC$ line and a proper electromechanical model which has been developed based on Hamilton's principle. The effect of tip loading in the equations of motion will also be considered. Our proposed modeling approaches will be validated based on the existing experimental data [14]. This model can be used both to optimize the open loop displacement of the actuator and to design advanced control systems [21–23], which will lead to practical uses of the actuator in micro/nanosystems.

## 1. The trilayer PPy actuator

In this paper, as an example of conjugated polymer actuators, the trilayer PPy actuator will be considered. Figure 1 depicts the trilayer PPy actuator. As the name indicates, the trilayer PPy actuator consists of three layers. The middle layer is porous polyvinylidene fluoride (PVDF) which is used as a storage tank for the electrolyte and on both sides of it there are polymer layers (PPy) [5, 6]. The electrolyte used is 0.1 M lithium trifluoromethanesulfonimide (Li$^+$TFSI$^-$) in the solvent propylene carbonate (PC, Aldrich) [14]. The thicknesses of the PPy and PVDF layers are approximately 22 $\mu$m and 110 $\mu$m respectively [14].

In general, both cations and anions can contribute to the actuation process. When polymer is prepared with small mobile anions and large cations, the diffusion of anions into the polymer dominates the actuation process and causes the
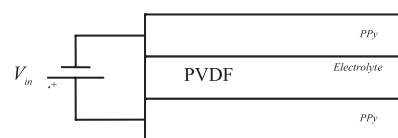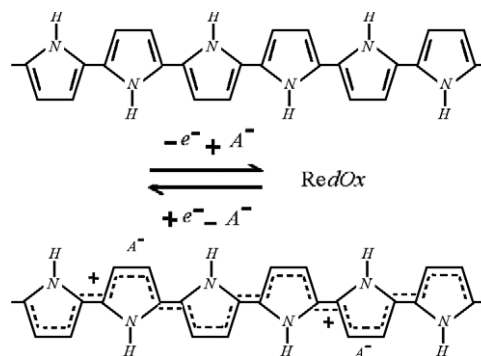


**Figure 1.** The three-layer PPy actuator.



**Figure 2.** The RedOx process in the polypyrrole actuator.

actuator to expand during oxidation. Alternatively, application of large anions and small mobile cations will cause the actuator to expand during reduction through the incorporation of cations. If the polymer is equipped with both mobile anions and cations, it will first expand and then contract during a change in oxidation state [14, 39, 4, 40, 41]. This undesirable process is called salt draining [42–44]. Therefore, the sizes of the ions play an important role in the dynamic response of conductive polymer actuators. It has been shown that the application of small mobile anions (TFSI$^-$) will improve the dynamic response of fast trilayer polymer actuators [14, 15]. Consequently the actuation process in these actuators will be primarily due to the diffusion of anions (TFSI$^-$) into the polymer. Figure 2 illustrates the RedOx process in polymer actuators where A$^-$ refers to anions.

Thus in the trilayer bender, while the PPy layer on the anode side is oxidized and expands as a result, the PPy layer on the cathode side is reduced and contracts. Therefore this difference in the volume will lead to the bending of the actuator.

## 2. Analytical multi-domain dynamic actuator model

The analytical multi-domain dynamic actuator (AMDDA) model is comprised of two parts, namely the electrochemical model and the electromechanical model.

### 2.1. Modeling assumptions

(1) The electrical and mechanical parameters of the model are time-invariant.
(2) There is no coupling between the mechanical and electrical models.
(3) The charge-to-strain ratio is linear and unidirectional.
(4) There is no degradation in the electrical or mechanical models.

**Table 1.** Definition of the physical parameters.

| Parameter | Definition |
| --- | --- |
| $D$ | Diffusion coefficient |
| $h$ | Thickness of the PPy layer |
| $R$ | Electrolyte and contact resistance |
| $\delta$ | Thickness of the double-layer capacitance |
| $I_t$ | Current |
| $V_{in}$ | Input voltage |
| $C_d$ | Double-layer capacitance |

(5) The actuator is isothermal.

(6) Considering the thickness of the PPy layers used in the experiments (11–29 $\mu$m) [14], the distribution of the induced stress can be assumed to be constant through the thickness [45].

(7) Based on the application of gold layers on both sides of the PVDF layer which diminishes the potential drop along the length of the actuator, the actuation characteristic of the PPy actuator is assumed to be uniform along its length. It must be noted that if the actuator is relatively long or it is not provided with gold layers this assumption may not be used.

(8) Considering the dimensions of the actuator, the Euler–Bernoulli beam theory will be used in mechanical modeling.

### 2.2. Electrochemical modeling

The electrochemical model relates the input voltage and chemical RedOx reaction inside the PPy actuator. The electrochemical process within a conductive polymer actuator can be modeled by means of an electrical circuit. The electrical charge can be stored within the actuator which is analogous to a capacitance element in an electrical circuit. Also the energy loss in the actuator can be modeled as an electrical resistance. Thus the simplest lumped electrical model which can describe the electrochemical process within a conductive polymer actuator is an $RC$ circuit [24]. It has been shown that the major mechanism which is responsible for ion transport within the conductive polymer actuator is diffusion [25, 26]. Considering the above assumption Madden [10] has proposed a continuum electrical admittance model for polymer actuators which is known as the diffusive elastic metal model (DEM). Fang *et al* [6, 27] obtained the electrical admittance model of a trilayer polymer actuator by utilizing the DEM. Equation (1) describes their proposed model; its physical parameters are illustrated in table 1. The electrical admittance model between the input voltage and the output current of the actuator is as follows:

$$\frac{I_t}{V_{in}} = \frac{1}{2} \frac{s[\frac{\sqrt{D}}{\delta}\tanh(h\sqrt{s/D}) + \sqrt{s}]}{\frac{\sqrt{s}}{C_d} + Rs^{3/2} + R\frac{\sqrt{D}}{\delta}s\tanh(h\sqrt{s/D})}. \qquad (1)$$

In this study we will derive the electrical admittance model of the actuator in a simple and straightforward way based on the uniform $RC$ transmission line model. It will be demonstrated that our electrical admittance model is analogous to the model of Fang *et al*. Several authors have proposed that
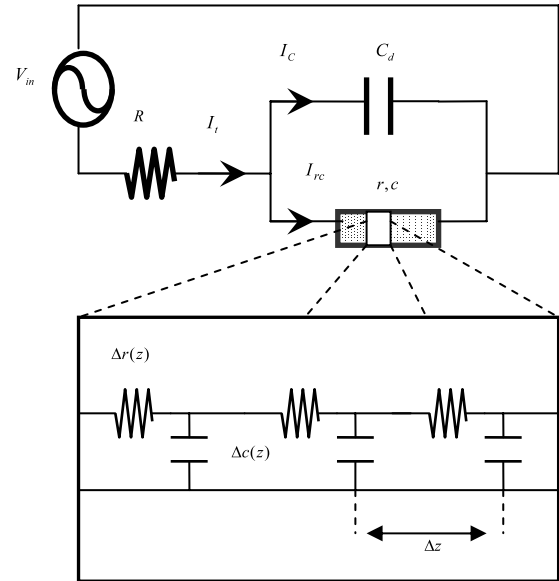


**Figure 3.** Description of the equivalent electrical circuit for the polymer actuator.

the transport of ions within the polymer can be modeled by a finite transmission line [28–32].

Figure 3 illustrates the equivalent electrical circuit model for a conductive polymer film which is in contact with electrolyte on one side. According to figure 3 we have represented the transport of ions with a finite $RC$ transmission line. $C_d$ is the double-layer capacitance at the polymer/electrolyte interface and $R$ is the electrolyte and contact resistance. The partial differential equation which governs a distributed $RC$ line is

$$\frac{\partial^2 V_{rc}(z,t)}{\partial z^2} = \frac{1}{rc}\frac{\partial V_{rc}(z,t)}{\partial t}, \qquad 0 \leqslant z \leqslant h \qquad (2)$$

where $r$ and $c$ are the resistance and capacitance per unit thickness of the polymer respectively. The general solution of equation (2) can be derived as

$$V_{rc}(z,s) = A\,\sinh(z\sqrt{s/\beta}) + B\cosh(z\sqrt{s/\beta}) \qquad (3)$$

where $\beta = \frac{1}{rc}$.

Also, suitable boundary conditions for the $RC$ transmission line in figure 3 can be defined as follows:

$$V_{in} - R[I_{rc}(0,s) + I_C] - V_{rc}(0,s) = 0 \qquad (4a)$$

$$I_{rc}(h,s) = 0 \qquad (4b)$$

where $I_{rc}(0,s)$ is the current in the distributed $RC$ line at the polymer/electrolyte interface, and $I_C$ is the double-layer charging current. Thus the voltage in the $RC$ transmission line can be obtained as

$$\frac{V_{rc}(z,s)}{V_{in}} = \frac{\cosh(z\sqrt{s/\beta}) - \tanh(h\sqrt{s/\beta})\sinh(z\sqrt{s/\beta})}{RC_d s + 1 + \frac{R}{r}\sqrt{s/\beta}\tanh(h\sqrt{s/\beta})}. \qquad (5)$$

We recall the relation between current and voltage in the transmission line:

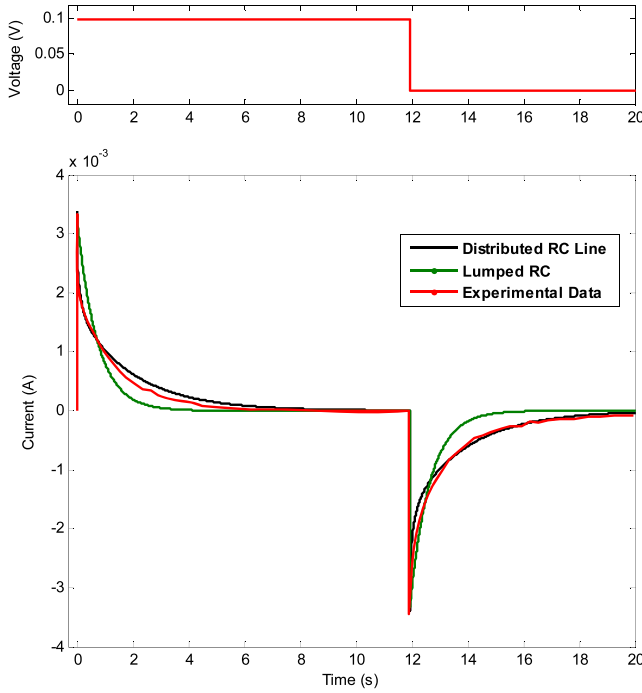$$I_{rc}(z,s) = \frac{-1}{r}\frac{\partial V_{rc}(z,s)}{\partial z}. \qquad (6)$$

**Figure 4.** Input voltage plus experimental and simulated current response of a 2 mm wide, 10 mm long fast trilayer polypyrrole bending actuator.



**Figure 5.** Description of the frame assignment for mechanical dynamic modeling.

### 2.3. Electromechanical modeling

The electromechanical model relates the input voltage and bending displacement of a PPy actuator. Three-layer polymer actuators can bend based on the expansion and contraction of the top and bottom layers. The induced stresses in the expanded or contracted layers are assumed to be the same and in the opposite directions. The distribution of induced stress is assumed to be approximately constant through the thickness. Additionally, application of gold layers on both sides of the PVDF layer diminishes the potential drop along the length of the actuator, thus the actuation characteristic of the actuator is uniform along its length. It was experimentally shown that the relation between the induced in-plane strain ($\varepsilon$) and the density of the transferred charges ($\rho$) is as follows [33]:

$$\varepsilon = \alpha\rho \tag{12}$$

where $\alpha$ is the strain-to-charge ratio, and $\rho$ can be achieved in the time domain as follows:

$$\rho(x, t) = [H(x) - H(x - L)]\frac{1}{bLh}\int_0^t I_t \, dt \tag{13}$$

where $H(x)$ is the Heaviside unit step function, $b$ is the width, $h$ is the thickness, and $L$ is the length of the PPy film. Now we will utilize Hamilton's principle to develop a suitable mechanical dynamic model for a trilayer polymer actuator with a point mass at its tip (figure 5).

Considering the dimensions of the actuator, it can be modeled based on the Euler–Bernoulli beam theory. The displacement field in this theory can be stated as follows [34]:

$$u_1(x, z, t) = -z\frac{\partial w(x, t)}{\partial x}$$
$$u_2(x, z, t) = 0 \qquad u_3(x, z, t) = w(x, t) \tag{14}$$

where $u_1$, $u_2$, and $u_3$ represent the displacement of a point $(x, y, z)$ along the $x$, $y$, and $z$ directions respectively and $w(x, t)$ is the displacement of any point in the $z$-direction. Thus for the small strain case one can derive the strain as

$$\varepsilon_x = \frac{\partial u_1}{\partial x} = -z\frac{\partial^2 w(x.t)}{\partial x^2}. \tag{15}$$

One can obtain the transmission line current as

$$\frac{I_{rc}(0, s)}{V_{in}} = \frac{\frac{1}{r}\sqrt{s/\beta}\tanh(h\sqrt{s/\beta})}{RC_d s + 1 + \frac{R}{r}\sqrt{s/\beta}\tanh(h\sqrt{s/\beta})}. \tag{7}$$

Furthermore, the double-layer charging current is

$$\frac{I_C}{V_{in}} = \frac{C_d s}{RC_d s + 1 + \frac{R}{r}\sqrt{s/\beta}\tanh(h\sqrt{s/\beta})}. \tag{8}$$

Finally the total current in the equivalent electrical circuits ($I_t = I_{rc}(0, s) + I_C$) will be derived as

$$\frac{I_t}{V_{in}} = \frac{s[\frac{c}{C_d}\sqrt{\beta}\tanh(h\sqrt{s/\beta}) + \sqrt{s}]}{\frac{\sqrt{s}}{C_d} + Rs^{3/2} + R\frac{c}{C_d}\sqrt{\beta}s\tanh(h\sqrt{s/\beta})}. \tag{9}$$

Thus equation (9) defines the electrical admittance model for a polymer film which is in contact with electrolyte on one side. Consequently for a trilayer polymer actuator the input voltage will be applied across two double-layer capacitances and the admittance is half of equation (9), that is,

$$Y(s) = \frac{1}{2}\frac{s[\frac{c}{C_d}\sqrt{\beta}\tanh(h\sqrt{s/\beta}) + \sqrt{s}]}{\frac{\sqrt{s}}{C_d} + Rs^{3/2} + R\frac{c}{C_d}\sqrt{\beta}s\tanh(h\sqrt{s/\beta})}. \tag{10}$$

Clearly equation (10) is analogous to equation (1) using the following transformation of variables:

$$\frac{C_d}{c} = \delta, \qquad \beta = D. \tag{11}$$

Figure 4 compares the existing experimental current output of the polymer actuator [14] with the lumped $RC$ model and distributed $RC$ line in response to a step voltage input. It is evident that the distributed model can perfectly predict the current response of the actuator.
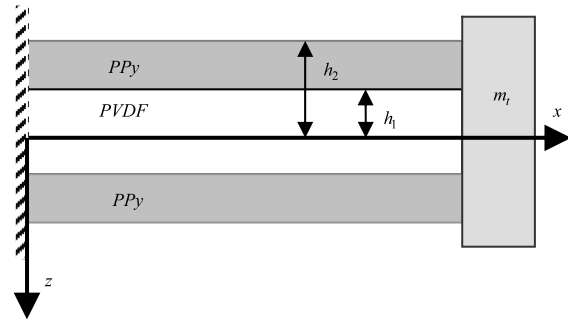
4

With this in mind, we can derive the actuator's equation of motion based on Hamilton's principle:

$$\int_{t_1}^{t_2} (\delta U + \delta V - \delta K)\, dt = 0 \qquad (16)$$

where $\delta U$ is the variation of the total strain energy, $\delta V$ is the variation of the potential energy of the applied forces on the external surfaces of the actuator, and $\delta K$ is the variation of the total kinetic energy. From the displacement field we have

$$
\delta U = \int_V \sigma_x \delta \varepsilon_x \, dV = \int_V \sigma_x \left[ -z \frac{\partial^2 \delta w}{\partial x^2} \right] dV
$$
$$
= \int_0^L \int_A \sigma_x \left[ -z \frac{\partial^2 \delta w}{\partial x^2} \right] dA\, dx = \int_0^L -\frac{\partial^2 \delta w}{\partial x^2} M_x \, dx
$$
$$
= \int_0^L -\frac{\partial^2 M_x}{\partial x^2} \delta w\, dx + \left[ \frac{\partial M_x}{\partial x} \delta w \right]_0^L - \left[ M_x \frac{\partial \delta w}{\partial x} \right]_0^L \quad (17)
$$

where $M_x = \int_A \sigma_x z \, dA$. Recalling the fact that only the PPy layers are electroactive and considering the Kelvin–Voigt damping model [35] for the actuator the stresses in the PVDF and PPy layers can be defined as follows:

$$\sigma_{x1} = E_1 \varepsilon_x + E_1^* \frac{\partial \varepsilon_x}{\partial t} \qquad (18a)$$

$$\sigma_{x2} = E_2 [\varepsilon_x - \alpha\, \rho(x,t)] + E_2^* \frac{\partial \varepsilon_x}{\partial t} \qquad (18b)$$

where $E_1$ and $E_2$ are the Young's moduli and $E_1^*$, and $E_2^*$ are the viscoelastic parameters of the PVDF and PPy layers respectively. Consequently the bending moment can be obtained as

$$
M_x = \int_A \sigma_x z \, dA = 2b \left[ \int_0^{h_1} E_1 \left( -z \frac{\partial^2 w}{\partial x^2} \right) z\, dz \right.
$$
$$
+ \int_0^{h_1} E_1^* \left( -z \frac{\partial^3 w}{\partial t \partial x^2} \right) z\, dz
$$
$$
+ \int_{h_1}^{h_2} E_2 \left( -z \frac{\partial^2 w}{\partial x^2} - \alpha\, \rho(x,t) \right) z\, dz
$$
$$
\left. + \int_{h_1}^{h_2} E_2^* \left( -z \frac{\partial^3 w}{\partial t \partial x^2} \right) z\, dz \right]
$$
$$
= -\frac{2b}{3} [E_1 h_1^3 + E_2 (h_2^3 - h_1^3)] \frac{\partial^2 w}{\partial x^2}
$$
$$
- \frac{2b}{3} [E_1^* h_1^3 + E_2^* (h_2^3 - h_1^3)] \frac{\partial^3 w}{\partial t \partial x^2} - M_c \quad (19)
$$

where

$$M_c = 2b \int_{h_1}^{h_2} E_2 \alpha \rho(x,t) z \, dz. \qquad (20)$$

The variation of the total kinetic energy of the polymer actuator can be derived as

$$
\delta K = \frac{1}{2} \int_0^L (\rho_1 A_1 + 2\rho_2 A_2) \left( \frac{\partial \delta w}{\partial t} \right)^2 dx + \frac{1}{2} m_t \left( \frac{\partial \delta w}{\partial t} \bigg|_{x=L} \right)^2
$$
$$(21)$$

where $\rho_1 A_1$ and $\rho_2 A_2$ are the products of density and cross-sectional area of the PVDF and PPy layers respectively, and $m_t$

is a point mass at the actuator's tip. Substituting equations (17) and (21) into Hamilton's principle gives us

$$
\int_{t_1}^{t_2} \left\{ \int_0^L \left[ (\rho_1 A_1 + 2\rho_2 A_2) \frac{\partial^2 w}{\partial t^2} - \frac{\partial^2 M_x}{\partial x^2} \right] \delta w\, dx \right.
$$
$$
- m_t \frac{\partial^2 w}{\partial t^2} \delta w \bigg|_{x=L} + \left[ \frac{\partial M_x}{\partial x} \delta w \right]_0^L
$$
$$
\left. - \left[ M_x \frac{\partial \delta w}{\partial x} \right]_0^L \right\} dt = 0. \qquad (22)
$$

Thus the governing equation of motion can be achieved as

$$
2b[\rho_1 h_1 + \rho_2 (h_2 - h_1)] \frac{\partial^2 w}{\partial t^2}
$$
$$
+ \frac{2b}{3} [E_1 h_1^3 + E_2 (h_2^3 - h_1^3)] \frac{\partial^4 w}{\partial x^4}
$$
$$
+ \frac{2b}{3} [E_1^* h_1^3 + E_2^* (h_2^3 - h_1^3)] \frac{\partial^5 w}{\partial t \partial x^4} + \frac{\partial^2 M_c}{\partial x^2} = 0 \quad (23)
$$

and the boundary conditions are

$$w(0,t) = 0, \qquad \frac{\partial w(0,t)}{\partial x} = 0, \qquad (24a)$$

$$M_x(L,t) = 0, \qquad \frac{\partial M_x(L,t)}{\partial x} - m_t \frac{\partial^2 w(L,t)}{\partial t^2} = 0. \quad (24b)$$

Up to now we have obtained the nonhomogeneous partial differential equation which governs the mechanical dynamics of fast trilayer polypyrrole bending actuators. In order to solve this equation, first we normalize it using the following transformation of variables:

$$\tilde{w} = \frac{w}{L}, \qquad \tilde{x} = \frac{x}{L}, \qquad \tilde{t} = \frac{t}{T}, \qquad \tilde{M}_c = \frac{M_c}{M} \quad (25)$$

where

$$T = L^2 \sqrt{\frac{3[\rho_1 h_1 + \rho_2 (h_2 - h_1)]}{E_1 h_1^3 + E_2 (h_2^3 - h_1^3)}} \qquad (26a)$$

$$M = \frac{2b}{3L} [E_1 h_1^3 + E_2 (h_2^3 - h_1^3)]. \qquad (26b)$$

Then, denoting

$$\gamma = \frac{E_1^* h_1^3 + E_2^* (h_2^3 - h_1^3)}{T[E_1 h_1^3 + E_2 (h_2^3 - h_1^3)]}, \qquad (27)$$

the normalized equation can be obtained as

$$\ddot{\tilde{w}} + \tilde{w}^{IV} + \gamma \dot{\tilde{w}}^{IV} + \tilde{M}_c'' = 0 \qquad (28)$$

where the superscript primes and dots denote derivatives with respect to $\tilde{x}$ and $\tilde{t}$ respectively. Next the Galerkin method will be used for solving equation (27). Based on this method the normalized output transverse displacement of the actuator can be approximated by $\psi(\tilde{x}, \tilde{t})$ [36, 37], where

$$\psi(\tilde{x}, \tilde{t}) = \sum_{i=1}^n \varphi_i(\tilde{x}) q_i(\tilde{t}) \qquad (29)$$

where $\varphi_i$ are an orthonormal set of eigenfunctions, which are associated with passive vibration of a fixed–free trilayer

polymer actuator with tip load and $q_i$ are time-dependent generalized coordinates. The normalized dynamics equation for passive vibration of the polymer actuator with a point mass at its tip is

$$\ddot{\psi} + \psi^{IV} = 0 \tag{30}$$

and the boundary conditions are

$$\psi(0, \tilde{t}) = 0, \qquad \psi'(0, \tilde{t}) = 0, \tag{31a}$$

$$\psi''(1, \tilde{t}) = 0, \qquad \psi'''(1, \tilde{t}) - \tilde{m}_t \ddot{\psi}(1, \tilde{t}) = 0 \tag{31b}$$

where

$$\tilde{m}_t = \frac{m_t}{2bL[\rho_1 h_1 + \rho_2(h_2 - h_1)]}. \tag{32}$$

One can use separation of variables for solving equation (30) by defining the following equality:

$$\psi(\tilde{x}, \tilde{t}) = \varphi(\tilde{x})q(\tilde{t}). \tag{33}$$

Substituting equation (33) into equation (30) leads to two ordinary differential equations:

$$\ddot{q} + \omega^2 q = 0 \tag{34}$$

$$\varphi^{IV} - \omega^2 \varphi = 0 \tag{35}$$

where $\omega$ are eigenvalues of equation (30), which will be obtained based on the following characteristic equation:

$$\cos(\beta_i)\cosh(\beta_i) + \beta_i \tilde{m}_t[\cos(\beta_i)\sinh(\beta_i)$$
$$- \cosh(\beta_i)\sin(\beta_i)] + 1 = 0 \tag{36}$$

where $\beta_i^4 = \omega_i^2$, and the corresponding eigenfunctions can be acquired as

$$\varphi_i(\tilde{x}) = \frac{[\sin(\beta_i) + \sinh(\beta_i)][\cosh(\beta_i \tilde{x}) - \cos(\beta_i \tilde{x})]}{\cosh(\beta_i)\sin(\beta_i) - \sinh(\beta_i)\cos(\beta_i)}$$
$$- \frac{[\cosh(\beta_i) + \cos(\beta_i)][\sinh(\beta_i \tilde{x}) - \sin(\beta_i \tilde{x})]}{\cosh(\beta_i)\sin(\beta_i) - \sinh(\beta_i)\cos(\beta_i)}. \tag{37}$$

Subsequently the orthogonality condition among the eigenfunctions will be derived. Considering that $\omega_i$ and $\omega_j$ are two distinct eigenvalues and $\varphi_i$ and $\varphi_j$ are their corresponding eigenfunctions, respectively, then from equation (34) we get

$$\varphi_i^{IV} - \omega_i^2 \varphi_i = 0 \tag{38}$$

$$\varphi_j^{IV} - \omega_j^2 \varphi_j = 0. \tag{39}$$

Multiplying equation (38) by $\varphi_j$ and equation (39) by $\varphi_i$ and integrating the subtracted result over the domain leads to

$$\int_0^1 (\varphi_i^{IV}\varphi_j - \varphi_j^{IV}\varphi_i) + (\omega_j^2 - \omega_i^2)\int_0^1 \varphi_i\varphi_j \, d\tilde{x} = 0. \tag{40}$$

Integration by parts twice gives us

$$[\varphi_i'''\varphi_j - \varphi_j\varphi_i''' - \varphi_i''\varphi_j' + \varphi_i'\varphi_j'']_0^1$$
$$+ (\omega_j^2 - \omega_i^2)\int_0^1 \varphi_i\varphi_j \, d\tilde{x} = 0. \tag{41}$$

Considering the boundary conditions in equation (31) the orthogonality condition can be simplified as [37]

$$\int_0^1 \varphi_i\varphi_j \, d\tilde{x} + \tilde{m}_t\varphi_i(1)\varphi_j(1) = \delta_{ij} \tag{42}$$

where $\delta_{ij}$ is the Kronecker delta. Substituting equation (29) into equation (28), multiplying by $\varphi_j$ and integrating over the domain we have

$$\sum_{i=1}^n [\ddot{q}_i + \gamma\omega_i^2\dot{q}_i + \omega_i^2 q_i][\delta_{ij} - \tilde{m}_t\varphi_i(1)\varphi_j(1)] - f_j(\tilde{t}) = 0,$$
$$j = 1, 2, \ldots, n \tag{43}$$

where

$$f_j(\tilde{t}) = -\int_0^1 \tilde{M}_c''\varphi_j \, d\tilde{x}$$
$$= -\alpha b E_2(h_2^2 - h_1^2)\frac{\bar{\rho}(\tilde{t})}{M}\int_0^1 [\delta'(0) - \delta'(1)]\varphi_j \, d\tilde{x}$$
$$= -\alpha b E_2(h_2^2 - h_1^2)\frac{\bar{\rho}(\tilde{t})}{M}\varphi_j'(1) \tag{44}$$

where $\delta(\cdot)$ represents the Dirac delta function and $\bar{\rho}(\tilde{t}) = (1/bLh)\int_0^{\tilde{t}} I_t \, d\tilde{t}$. Equation (43) shows that the mechanical dynamics of a fast trilayer polypyrrole bending actuator with tip loading can be modeled with $n$ coupled ordinary differential equations. We can rewrite the equation (43) in the matrix form as follows:

$$\{\ddot{q}(\tilde{t})\} + \gamma\Lambda\{\dot{q}(\tilde{t})\} + \Lambda\{q(\tilde{t})\} - A^{-1}\{f(\tilde{t})\} = 0 \tag{45}$$

where $A$ is an $n \times n$ symmetrical matrix with elements $A_{ij} = \delta_{ij} - \tilde{m}_t\varphi_i(1)\varphi_j(1)$ and $\Lambda$ is an $n \times n$ diagonal matrix with elements $\Lambda_{ij} = \omega_i^2\delta_{ij}$. To obtain the transfer function of the system we apply the Laplace operator to equation (45), which leads to

$$\{Q(s)\} = [Is^2 + \gamma\Lambda s + \Lambda]^{-1}A^{-1}\{F(s)\} \tag{46}$$

where $I$ is an $n \times n$ unit matrix. Furthermore $\{Q(s)\}$ and $\{F(s)\}$ are the Laplace transform of $\{q(\tilde{t})\}$ and $\{f(\tilde{t})\}$ respectively. Substituting equation (46) into equation (29) will introduce the transfer function of equation (28). Having this in mind the output displacement of the actuator based on equation (23) can be derived as follows:

$$w(x, s) = LT\sum_{i=1}^n \varphi_i\left(\frac{x}{L}\right)Q_i(Ts). \tag{47}$$

## 3. Results and discussion

Most of the previously reported models in the literature of conductive polymer actuators have focused on steady state operating conditions [17, 18, 24, 38]. Fang *et al* [6] have proposed a dynamic model for trilayer PPy actuators. However, their model was based on the electrochemical dynamics of the actuator and cannot take into account the mechanical dynamics; therefore it is not suitable for predicting the dynamic behavior of fast trilayer PPy actuators. In this study as a step forward in understanding the dynamic behavior of fast trilayer PPy actuators we have developed a complete electro-chemo-mechanical dynamic model between the input voltage and the output displacement of the actuator. This model is based on the physical parameters of the actuator and can be used to optimize the open loop displacement of the
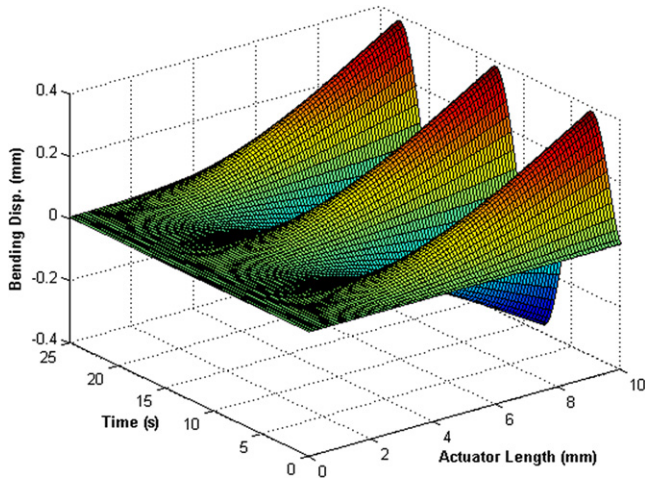
**Figure 6.** Actuator displacement over its whole length in response to a sine wave input voltage.
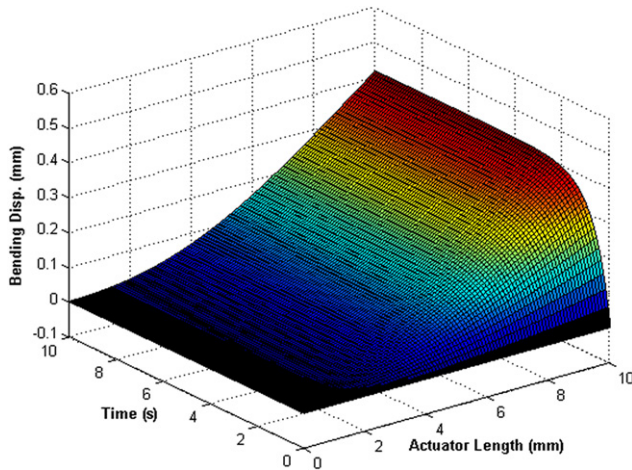


**Figure 7.** Actuator displacement in response to a step input voltage for the whole actuator length.



**Figure 8.** Input voltage plus experimental and simulated output displacement response of a 2 mm wide, 10 mm long fast trilayer polypyrrole bending actuator.



**Figure 9.** Dynamic displacement response of a 2 mm wide, 10 mm long fast trilayer polypyrrole bending actuator.

actuator. In order to validate the proposed dynamic model, the available published experimental results [14] are employed. This is done based on the experimental data of a 2 mm wide, 10 mm long fast trilayer polypyrrole bending actuator. Both time and frequency domain simulation results will be presented in order to evaluate our proposed dynamic model. Figure 6 illustrates the actuator displacement through the whole length in response to a sine wave input voltage. From this figure it is evident that the fixed–free boundary condition is satisfied. Figure 7 depicts the actuator displacement in response to a step input voltage for the whole actuator length. Based on the available experimental data [14], figure 8 compares the simulated and experimental output displacements of the actuator in response to a step voltage input. It is evident that the model shows a relatively good match with the experimental results. Figure 9 compares the Bode plot of the experimental results reported in [14] with the response of our theoretical model, which indicates that the purposed model can predict the frequency domain behavior of the actuator well. We have also considered the effects of tip load variation which
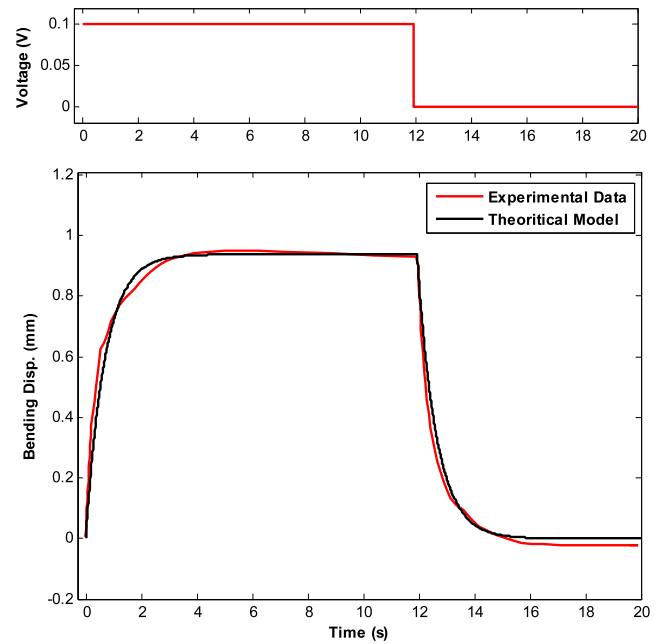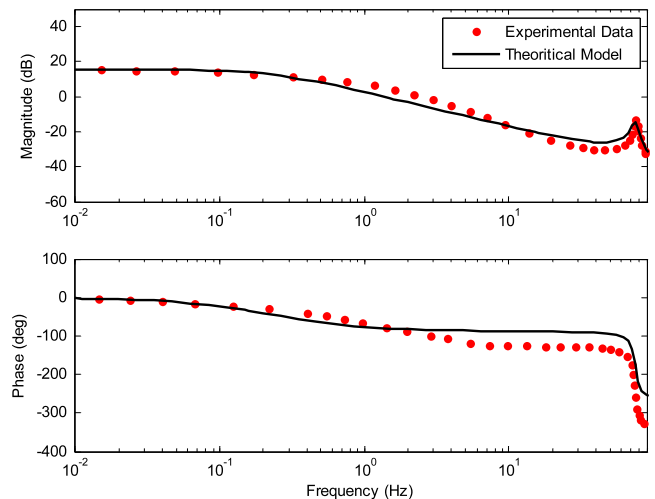
can be important in practical applications of the actuator in functional devices. According to figure 10 increase of the tip mass will decrease the fundamental natural frequency, which is consistent with the reported experimental data [14].

## 4. Conclusions

In this paper, a complete analytical dynamic model of the input voltage and output displacement of a fast trilayer polypyrrole bending actuator is proposed (AMDDA). Consideration is given to the tip loading conditions. The electrical admittance model of a trilayer bender has been obtained based on a distributed $RC$ line which matches well with the existing
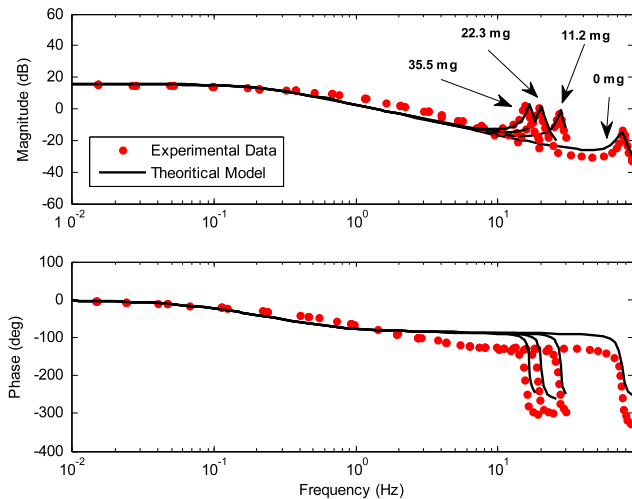
**Figure 10.** Dynamic displacement response of a 2 mm wide, 10 mm long fast trilayer polypyrrole bending actuator with 0, 11.2, 22.3, and 35.5 mg tip masses.

experimental results. Utilizing Hamilton's principle it has been shown that the mechanical dynamics of the actuator can be modeled with a nonhomogeneous partial differential equation. The dynamics equation of motion has been solved by means of the Galerkin method and the obtained results have been compared with published experimental results. It has been shown that the proposed model can consistently predict the dynamic behavior of the actuator in both the time and the frequency domain. This model can be used both to optimize the open loop displacement of the actuator and to design a proper controller, which will lead to practical uses of the actuator in micro/nanosystems. The developed model not only satisfies a fast trilayer polymer actuator but is a proper choice for devices that utilize conductive polymer materials. The proposed model can be considered as a step forward in understanding the dynamic behavior of conducting polymer actuators based on their physical parameters.

## Acknowledgments

## References

[1]   Hollerbach J M, Hunter I W and Ballantyne J 1999 *A Comparative Analysis of Actuator Technologies for Robotics* (Cambridge, MA: MIT Press)

[2]   Hunter I W and Lafontaine S 1992 A comparison of muscle with artificial actuators *Solid-State Sensor and Actuator Workshop, 5th Technical Digest* (Piscataway, NJ: IEEE)

[3]   Bar-Cohen Y (ed) 2001 *Electroactive Polymer (EAP) Actuators as Artificial Muscles: Reality, Potential, and Challenges* (Bellingham, WA: SPIE Optical Engineering)

[4]   Smela E 2003 Conjugated polymer actuators for biomedical applications *Adv. Mater.* **15** 481–94

[5]   Wallace G and Spinks G 2007 Conducting polymers–bridging the bionic interface *Soft Matter* **3** 665–71

[6]   Fang Y *et al* 2008 A scalable model for trilayer conjugated polymer actuators and its experimental validation *Mater. Sci. Eng.* **28** 421–8

[7]   Della Santa A, De Rossi D and Mazzoldi A 1997 Characterization and modeling of a conducting polymer muscle-like linear actuator *Smart Mater. Struct.* **6** 23–34

[8]   Smela E, Inganas O and Lundstrom I 1995 Controlled folding of microsize structures *Science* **268** 1735–8

[9]   Kaneto K, Kaneko M, Min Y and MacDiarmid A G 1995 Artificial muscle: electromechanical actuators using polyaniline films *Synth. Met.* **71** 2211–2

[10]   Madden J D 2000 Conducting polymer actuators *PhD Thesis* MIT

[11]   Chen Z, Shatara S and Tan X 2010 Modeling of biomimetic robotic fish propelled by an ionic polymer–metal composite caudal fin *IEEE/ASME Trans. Mechatronics* vol 15 pp 448–59

[12]   Jager E W H, Smela E and Ingana O 2000 Microfabricating conjugated polymer actuators *Science* **290** 1540–5 (www.sciencemag.org)

[13]   Amiri Moghadam A A, Moavenian M and Tousi H E 2011 Modeling and robust control of a soft robot based on conjugated polymer actuators *Int. J. Modell. Identif. Control* **14** 216–26

[14]   John S W 2008 Modelling and control of conductive polymer actuators *PhD Thesis* University of Wollongong

[15]   Wu Y *et al* 2006 Fast trilayer polypyrrole bending actuators for high speed applications *Synth. Met.* **156** 1017–22

[16]   John S W *et al* 2008 Validation of resonant frequency model for polypyrrole trilayer actuators *IEEE/ASME Trans. Mechatronics* **13** 401–9

[17]   Santa A D, De Rossi D and Mazzoldi A 1997 Characterization and modelling of a conducting polymer muscle-like linear actuator *Smart Mater. Struct.* **6** 23–34

[18]   Christophersen M, Shapiro B and Smela E 2006 Characterization and modelling of PPy bilayer microactuators. Part 1. Curvature *Sensors Actuators* B **115** 596–609

[19]   Madden J D, Cush R A, Kanigan T S and Hunter I W 2000 Fast contracting polypyrrole actuators *Synth. Met.* **113** 185–92

[20]   Amiri Moghadam A A, Torabi K and Moavenian M 2011 Finite element modeling and robust control of fast trilayer polypyrrole bending actuators *Int. J. Appl. Electromagn. Mech.* **35** 281–305

[21]   Amiri Moghadam A A and Tootoonchi A A 2010 Multi-level fuzzy-QFT control of conjugated polymer actuators *Proc. 41st Int. Symp. on Robotics (ISR) and 6th German Conf. on Robotics (ROBOTIK) (Munich, Germany, 7–9 June 2010)* pp 1038–45

[22]   Amiri Moghadam A A, Moavenian M and Torabi K 2010 Takagi–Sugeno fuzzy modelling and parallel distribution compensation control of conducting polymer actuators *J. Syst. Control Eng.* **224** 41–51

[23]   Torabi K, Moavenian M, Amiri Moghadam A A and Amiri Moghadam A H 2009 Modelling and control of conjugated polymer actuators using robust control QFT *17th Annu. Int. Conf. on Mechanical Engineering (ISME)* pp 201–8

[24]   Madden P G A 2003 Development and modeling of conducting polymer actuators and the fabrication of a conducting polymer based feedback loop *PhD Thesis* Massachusetts Institute of Technology

[25]   Daum P, Lenhard J R, Rolison D and Murray R W 1980 Diffusional charge transport through ultrathin films of radiofrequency plasma polymerized vinylferrocene at low temperature *J. Am. Chem. Soc.* **102** 4649–53

[26] Amemiya T, Hashimoto K and Fujishima A 1993
Frequency-resolved faradaic processes in polypyrrole films
observed by electromodulation techniques: electrochemical
impedance and color impedance spectroscopies *J. Phys.
Chem.* **97** 4187–91

[27] Fang Y *et al* 2008 Robust adaptive control of conjugated
polymer actuators *IEEE Trans. Control Syst. Technol.*
**16** 600–12

[28] Madden J D W, Madden P G A and Hunter I W 2002
Conducting polymer actuators as engineering materials
*Proc. SPIE 9th Annual Symp. on Smart Structures and
Materials: Electroactive Polymer Actuators and Devices*
ed B-C Yoseph (San Diego, CA: SPIE) pp 176–90

[29] Warren M 2005 Electronic and structural effects on the
electrochemistry of polypyrrole *Masters Thesis*

[30] Tso C H, Madden J D W and Michal C A 2007 An NMR study
of PF6-ions in polypyrrole *Synth. Met.* **157** 460–6

[31] Punning A 2007 Electromechanical characterization of ion
polymer metal composite sensing actuators *PhD
Dissertation* Department of Physics, Tartu University,
Estonia

[32] Lashidani T S H 2010 Engineering aspects of polypyrrole
actuator and their application in active catheters *PhD Thesis*
University of British Columbia

[33] Otero T F and Sansinena J M 1997 Bilayer dimensions and
movement inartificial muscles *Bioelectrochem. Bioenerget.*
**42** 117–22

[34] Reddy J N 2003 *Mechanics Of Laminated Composite Plates
And Shells* 2nd edn (Boca Raton, FL: CRC Press)

[35] de Silva C W 2000 *Vibration: Fundamentals and Practice*
(Boca Raton, FL: CRC Press LLC)

[36] Kelly S G 2007 *Advanced Vibration Analysis* (London: Taylor
and Francis)

[37] Meirovitch L 1986 *Elements of Vibration Analysis* 2nd edn
(New York: McGraw-Hill)

[38] Du P, Lin Xi and Zhang X 2010 A multilayer bending model
for conducting polymer actuators *Sensors Actuators* A
**163** 240–6

[39] Madden P G A, Madden J D W, Anquetil P A, Vandesteeg N A
and Hunter I W 2004 The relation of conducting polymer
actuator material properties to performance *IEEE J. Ocean.
Eng.* **29** 696–705

[40] Skaarup S, Bay L, Vidanapathirana K, Thyboa S, Toftea P and
Westb K 2003 Simultaneous anion and cation mobility in
polypyrrole *Solid State Ion.* **159** 143–7

[41] Vandesteeg N, Madden P G, Madden J D, Anquetil P A and
Hunter I W 2003 Synthesis and characterization of
EDOT-based conducting polymer actuators *EAPAD:
Electroactive Polymer Actuators and Devices*; *Proc. SPIE*
**5051** 349–56

[42] Pei Q and lnganas O 1992 Electrochemical application of the
bending beam method: 1. Mass transport and volume
changes in polypyrrole during redox *J. Phys. Chem.*
**96** 10507–14

[43] Pei Q and lnganas O 1993 Electrochemical application of the
bending beam method: 2. Electroshrinking and slow
relaxation in polypyrrole *J. Phys. Chem.* **97** 6034–41

[44] Gandhi M, Murray P, Spinks G and Wallace G 1995
Mechanism of electromechanical actuation in polypyrrole
*Synth. Met.* **73** 247–65

[45] Metz Ph *et al* 2006 A finite element model for bending
behaviour of conducting polymer electromechanical
actuators *Sensors Actuators* A **130** 1–11